Applied Catalysis B: Environmental 125 (2012) 120–127

Contents lists available at SciVerse ScienceDirect

Applied Catalysis B: Environmental

journal homepage: www.elsevier.com/locate/apcatb

Electro-Fenton oxidation of pesticides with a novel Fe_3O_4@Fe_2O_3/activated carbon aerogel cathode: High activity, wide pH range and catalytic mechanism

Hongying Zhao[a,b], Yujing Wang[a], Yanbin Wang[a], Tongcheng Cao[a,b], Guohua Zhao[a,b,*]

[a] Department of Chemistry, Tongji University, 1239 Siping Road, Shanghai 200092, PR China
[b] Key Laboratory of Yangtze River Water Environment, Ministry of Education, Tongji University, 1239 Siping Road, Shanghai 200092, PR China

ARTICLE INFO

Article history:
Received 25 January 2012
Received in revised form 2 May 2012
Accepted 27 May 2012
Available online 4 June 2012

Keywords:
Composite iron oxide
Activated carbon aerogel electrode
Electro-Fenton
Surface reaction
Imidacloprid

ABSTRACT

A novel electro-Fenton (E-Fenton) system with the Fe_3O_4@Fe_2O_3/activated carbon aerogel (ACA) composite cathode was firstly constructed in this study. Its application on degrading imidacloprid exhibited highly catalytic efficiency over a wide applicable pH range from 3 to 9. The removal of imidacloprid and TOC achieved to 90% within 30 and 60 min, respectively. The nature of composite cathode was examined by BJH, XRD, SEM, TEM, XPS and FTIR techniques. ACA with high surface area of 2410 $m^2\ g^{-1}$ and multiplicated porosities composed of micropores and mesopores worked not only as cathode but also as Fenton catalyst support, enhancing oxidation activity. We proposed reasonable E-Fenton oxidation mechanisms with Fe_3O_4@Fe_2O_3/ACA cathode at acidic and basic conditions. At pH 3, it followed a Haber–Weiss mechanism that the dissolved iron ions and surface Fe(II) sites catalyzed the decomposition of H_2O_2 to generate hydroxyl radicals (•OH). While at pH 9, it was expected the formation and deactivation of H_2O_2 complex as well as the catalytic decomposition of H_2O_2 with surface Fe(III) and Fe(II) sites to produce both superoxide anion ($•O_2^-$/$HO_2•$) and hydroxyl radicals (•OH), involving an in situ recycling of iron oxide ($FeO{\cdot}Fe_2O_3 \rightarrow Fe_2O_3$).

1. Introduction

Fenton and related reactions encompass reactions of hydrogen peroxide with iron ions to form active oxygen species that oxidize organic or inorganic compounds when there are present [1,2]. The reactions have become of great interest for their relevance to the treatment of hazardous wastes [3,4]. During this process, hydroxyl radicals (•OH) are produced through various reactions between ferrous ions (Fe^{2+}) and hydrogen peroxide (H_2O_2) [4], as shown in Eq. (1).

$$H_2O_2 + Fe^{2+} \rightarrow Fe^{3+} + OH^- + {}^{\bullet}OH \quad (1)$$

However, despite its high efficiency, the wide application of traditional Fenton process is limited by its acidic pH requirement (pH 2–3) and the formation of iron sludge in the coagulation strep [5]. Meanwhile, Fe^{2+} (or Fe^{3+}) ions could not be recycled, which brings a new contamination. Therefore, the development of extending working pH range of Fenton reaction from strongly acidic condition to neutral, even basic ones is of great importance. Supported or immobilized heterogeneous Fenton catalysts (e.g. goethite, hematite, magnetite supported on silica and alumina) with high activity were successfully developed to these purposes [6,7]. It appears that supports could improve the performance of heterogeneous iron-containing catalysts. Very recently, more and more attentions have been attracted that deal with refractory organic pollutants in waters over wide pH ranges by means of heterogeneous electro-Fenton (E-Fenton) methods with supported Fenton catalysts [8,9]. Compared with classic Fenton systems, the E-Fenton systems can avoid the addition of expensive H_2O_2 and instiu electro-generate H_2O_2 by O_2 reduction on cathodal electrodes (Eq. (2)) with the regeneration of Fe^{2+} by a direct cathodal reaction (Eq. (3)) as follows [10–12]:

$$O_2 + 2H^+ + 2e \rightarrow H_2O_2 \quad (2)$$

$$Fe^{3+} + e \rightarrow Fe^{2+} \quad (3)$$

The understanding of catalytic mechanism through which it efficiently works over a wide pH range relatively becomes important. Some investigators suggested that the activation of H_2O_2 by iron oxides was followed by Haber–Weiss mechanism (series 1e transfer step) whether under acidic or neutral condition [13]. The oxidation of organic contaminants has been attributed to •OH producing from the reaction of H_2O_2 with dissolved iron ion (Fe^{2+}) and/or surface iron (Fe(II)) [13]. Oppositely, Lin and Gurol [14] argued that the Weiss mechanism cannot appropriately describe the reaction mechanism for decomposition of H_2O_2 over surface of iron oxides. Alternatively, other investigators also pointed that the

* Corresponding author at: Department of Chemistry, Tongji University, 1239 Siping Road, Shanghai 200092, PR China. Tel.: +86 21 65988570; fax: +86 21 65982287.
E-mail address: g.zhao@tongji.edu.cn (G. Zhao).

0926-3373/$ – see front matter © 2012 Elsevier B.V. All rights reserved.
http://dx.doi.org/10.1016/j.apcatb.2012.05.044

decomposition of H_2O_2 on the surface of iron oxides at neutral pH values may proceed mainly through a non-radical mechanism (2e transfer step) that converts H_2O_2 directly into O_2 and H_2O without the production of $^{\bullet}OH$ [15]. Possibly, this is due to the fact that surface reactivities of iron oxides would be different for each type of iron oxide.

Therefore, based on E-Fenton system, the aim of this work was to (i) produce an effectively heterogeneous and supported E-Fenton catalyst which can extend the pH range to neutral even to basic condition, (ii) investigate the corresponding catalytic oxidation mechanism of E-Fenton process with heterogeneous Fenton catalyst over wide pH ranges. For this purpose, the composite iron oxide containing both hematite and magnetite was prepared as Fenton catalyst, while the novel activated carbon aerogel with high surface area of 2410 $m^2\,g^{-1}$ was synthesized not only as catalyst support but also as cathode. Imidacloprid was selected as a model target contaminant for assessing the catalytic activity of this system because it is respective of a wide range of modern pesticides and highly soluble in water (of special interest because of their extremely easy transport in environment, seriously threatening all surface and ground water) [16,17]. In addition, numerous studies demonstrated that Fenton and Fenton-assisted methods are effective process for removing pesticides in wastewater [18,19]. Thus, it is reasonable to apply E-Fenton process with this novel cathode for effectively degrading imidacloprid in this work. Additionally, the corresponding mechanism was studied in detail through the role of participant oxidants, surface properties and reactions revealed by the comprehensive characterizations.

2. Experimental

2.1. Preparation and characterization of Fe_3O_4@Fe_2O_3/ACA composite cathode

Resorcinol, formaldehyde, sodium carbonate, acetone, ethyl alcohol, sodium hydroxide, iron sulfate, hydrazine hydrate, dimethyl sulfoxide, isopropanol, benzoquinone and imidacloprid were obtained from Aladdin Co., China and polyvinylpyrrolidone (PVP) was obtained from Aldrich. All of the chemicals were reagent grade and used without further purification. The activated carbon aerogel (ACA) was prepared according to a modified ambient drying technique described in our previous work [20,21], including sol–gel formation, solvent exchange, ambient pressure drying and pyrolysis. Specially in the present study, the pyrolysis was kept at 850 °C for 4 h in the mixture of carbon dioxide and argon (1:3, v/v) with the flow rate of 200 mL min^{-1} and heating rate of 5 °C min^{-1}. The composite iron oxide/ACA cathode (denoted by Fe_3O_4@Fe_2O_3/ACA) was synthesized through a typical hydrothermal method [22] with stoichiometric $FeSO_4{\cdot}7H_2O$ as precursor, $N_2H_4{\cdot}H_2O$ as reducer and PVP (K-30; MW = 40 000) as capping polymer. The solution was adjusted to pH 9 by NaOH, and then hydrothermally treated at 180 °C in a Teflon-lined stainless-steel autoclave for 22 h. Finally, the gained electrode was washed three times separately with ethanol and distilled water, and then dried at 60 °C for 6 h.

The surface area and pore sizes of ACA was measured by nitrogen adsorption at 77 K on a Micromeritics 3000 apparatus after heat treatment under vacuum at 573 K for 3 h. The X-ray diffraction (XRD) measurements were carried out on a Rigaku-D/max2550 powder diffractometer with Cu Kα radiation (at 40 kV, 30 mA over the 2θ range 3–80°). The X-ray photoelectron spectra were measured on an EScalab 250Xi spectrometer equipped with XR6 mononchromated X-ray source. Infrared (IR) spectra were recorded on a Bruker VERTEM 70 FTIR spectrometer using the KBr pellet technique. The morphology and microstructure were characterized by using scanning electron microscopy (SEM, Hitachi-S4800) and transmission electron microscopy (TEM, JEOL-JEM2100) with an accelerating voltage of 200 kV.

2.2. Apparatus and analysis procedures

Degradation experiment was carried out in a cylindrical single-compartment cell. The reactor was externally connected to circulating water to keep the reaction at constant temperature of 25 °C. The anode was a 4.5 cm^2 BDD thin film deposited on a conductive Si sheet purchased from Switzerland. A cathode with the same surface area was used and the gap between the electrodes was 2 cm. During the reaction, pure oxygen at 0.02 $m^3\,h^{-1}$ was insufflated into the cell through a porous pipe-diffuser placed right under the cathode with constant current density of 10 mA cm^{-2}. Imidacloprid solution (50 mL, 236.7 mg L^{-1}) was degraded in an aqueous medium containing 0.05 M Na_2SO_4 as supporting electrolyte. Specially, for homogeneous E-Fenton system, 1 mM $FeSO_4$ was used as catalyst. Before each analysis, samples aliquots withdrawn from treated solutions were filtered with 0.45 μm PTFE filters.

The concentration of imidacloprid during the E-Fenton oxidation process was analyzed by reversed-phase HPLC chromatography (Agilent HP 1100, Agilent Corporation, USA) at room temperature equipped with Agilent AQ-C18 column (4.6 mm × 150 mm × 5 μm) and selected photodiode detector at λ = 270 nm. The mobile phase was a mixture of methanol and water (30:70, v/v) with a flow rate of 1.0 mL min^{-1}. The hydroxyl radicals were determined with a simple and sensitive method which has been widely reported in the literatures [23–25]. The proposed method employed the reaction between hydroxyl radicals and dimethyl sulfoxide (DMSO) was generated quantitatively formaldehyde, which then reacted with 2,4-dinitrophenylhydrazine (DNPH) to form the corresponding hydrazine (HCHO-DNPH) and further analyzed by HPLC (Agilent HP 1100, Agilent). An Agilent Zorbax Eclipse XDB-C18 column (150 mm × 4.6 mm × 5 μm) was used at room temperature and with selected UV detector at λ = 355 nm. To perform the isocratic elution at a flow rate of 1.0 mL min^{-1}, a mixture of methanol and water (60:40, v/v) was used as mobile phase. Specially, the determination of hydroxyl radicals generated on cathode was carried out in a divided system with 250 mM DMSO. The content of Fe^{3+} was obtained from the light absorption of their corresponding colored complexes with SCN^- at λ = 466 nm [26]. Total organic carbon (TOC) was measured on a Shimadzu TOC-Vcpn analyzer.

3. Results and discussion

3.1. Catalytic performance of E-Fenton system with Fe_3O_4@Fe_2O_3/ACA cathode over wide pH ranges

Fig. 1A plots the imidacloprid degradation efficiency of traditional homogeneous E-Fenton technique with ACA cathode (Fe^{2+}/ACA) and heterogeneous E-Fenton methods with novel Fe_3O_4@Fe_2O_3/ACA cathode at optimal pH 3, while Fig. 1B presents the effect of pH on TOC removal in these two E-Fenton systems. As shown in Fig. 1A, imidacloprid was degraded rapidly both in Fe_3O_4@Fe_2O_3/ACA and Fe^{2+}/ACA processes, and the removal of imidacloprid achieved 90% within 30 min. The efficiency is mostly due to the excellent characteristics of adsorption, conductivity and catalysis of ACA cathode with extremely high surface area of 2410 $m^2\,g^{-1}$, which can efficiently generate H_2O_2 during electrochemical (EC) process. The N_2 adsorption–desorption isotherms and pore size distribution of ACA sample is depicted in Fig. 2. It should be note that, after activation, ACA possesses porosities composed of both micropores and mesopores with size centered at 1.7 and 3.5, respectively (see Fig. 2, inset). The oxidation behavior of

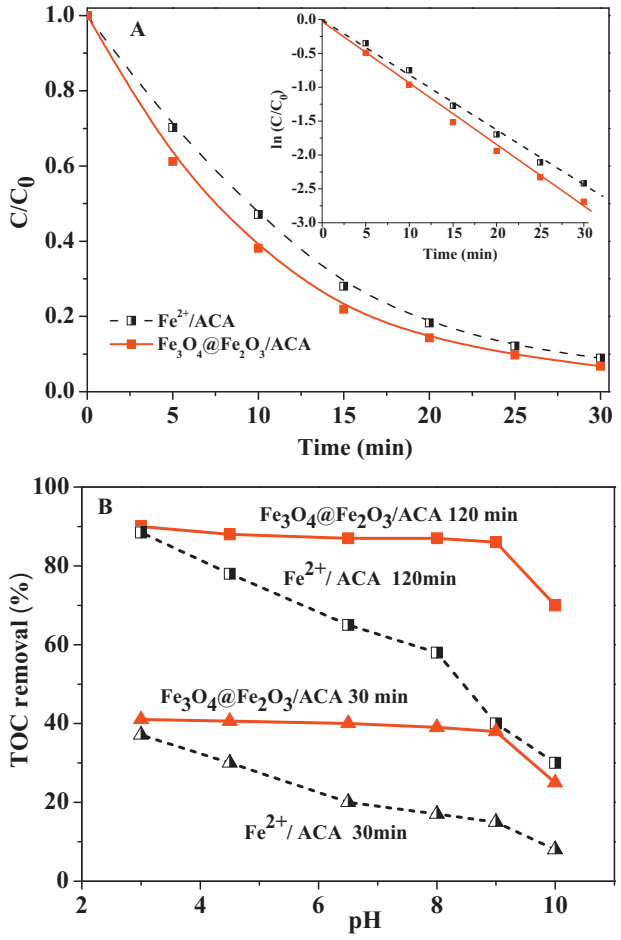

Fig. 1. (A) Catalytic degradation of imidacloprid at pH 3 and (B) the effect of pH on TOC removal after 30 and 60 min degradation time in different electro-Fenton systems.

cathode Fe_3O_4@Fe_2O_3/ACA is determined not only by the properties of used iron oxide but also by the porous texture of the support ACA. Microporosity strongly favored the imidacloprid adsorption capacity and tended to reduce the metal leaching, while mesoporosity strongly increased the metal dispersion [27]. This is why Fe_3O_4@Fe_2O_3/ACA E-Fenton method exhibited higher catalytic activity than traditional E-Fenton system with Fe^{2+}. In addition, the imidacloprid degradation reaction was observed to approximately follow a pseudo-first-order kinetic model (see inset of Fig. 1A), the kinetic constant of Fe_3O_4@Fe_2O_3/ACA was 0.091 min^{-1}, being a little bit higher of that (0.084 min^{-1}) in typical Fe^{2+}/H_2O_2 system.

The total organic carbon (TOC) in reaction solution was measured as an indicator for the organic mineralization at different time intervals. Fig. 1B shows the removal of TOC separately after 30 and 60 min reaction time at a wide pH range of 3–10 in the two E-Fenton systems. Obviously, heterogeneous Fe_3O_4@Fe_2O_3/ACA E-Fenton system was exhibited to be satisfactory over a wider pH ranges compared to Fe^{2+}/ACA. It was observed that 41% of TOC removal was reached at 30 min and then notably increased to 90% after 120 min at a very wide pH values from 3 to 9. Only when increasing pH to 10, a quick decline of TOC removal was observed both after 30 and 120 min of electrolysis. This is mostly due to the fast decomposition of H_2O_2 into H_2O and O_2 at strong basic conditions and/or due to the decreasing of the adsorption of H_2O_2 on the catalyst covered with Fe(III) complexes [28]. For conventional Fe^{2+}/ACA process, although similar TOC removal was observed with Fe_3O_4@Fe_2O_3/ACA at pH 3 (at 30 min: 37%; at 120 min 39%), its performance declined obviously with increasing pH value. For example, TOC removal at 120 min was decreased to 58% at pH 8, 40% at pH 9 and 30% at pH 10. These results further prove that this novel E-Fenton system with Fe_3O_4@Fe_2O_3/ACA cathode is feasible within wide pH ranges from 3 to 9 without sacrificing efficiency.

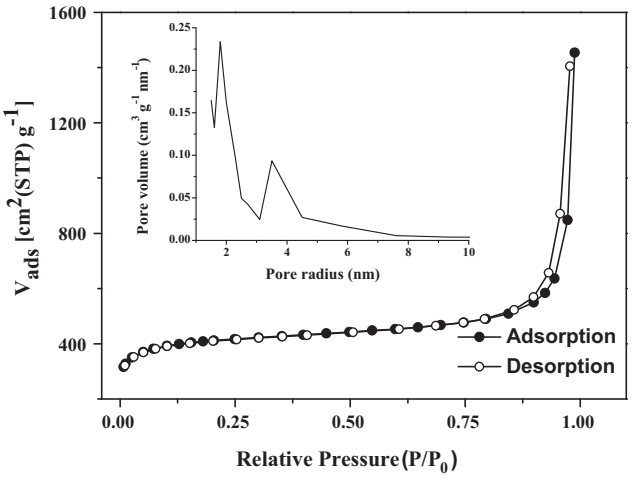

Fig. 2. N_2 adsorption isotherms of activated aerogel cathode (activated 4 h). The corresponding pore size distribution is depicted in the inset plot.

3.2. Detection of generated oxidants and leached iron ions during E-Fenton process

Since hydroxyl radical and leached iron ions are crucial parameters for understanding the efficiency of E-Fenton reaction, we measure the concentrations of •OH and Fe^{3+} in efficient and stable heterogeneous E-Fenton system at different pH values, as respectively presented in Fig. 3A and B. Both •OH and Fe^{3+} concentration obviously increased with extending pH value, especially from pH 6.5 to 3. In another word, the hydroxyl radicals and ferric iron were produced through the Fenton process (see Eq. (1)) between ferrous iron and electro-generated H_2O_2 at optimum pH 3. That is why both the amount of Fe^{3+} and •OH at pH 3 remain highest. Besides the dissolved iron ions, surface iron sites could also react with H_2O_2 to generate •OH, which will be discussed in the following oxidation mechanism part. However, almost no iron ions were detected in basic condition during the whole E-Fenton process, indicating a completely surface-catalyzed process for H_2O_2 decomposition. All these observation indicated that the oxidation mechanism of Fe_3O_4@Fe_2O_3/ACA E-Fenton system in acid and basic solution would be different. So how pH values determine participant oxidants generated during the decomposition of H_2O_2 by Fe_3O_4@Fe_2O_3 catalyst was deeply studied as follows.

Moreover, the oxidants generated from the decomposition of H_2O_2 could be hydroxyl (•OH) and/or superoxide anion ($•O_2^-$), the conjugate base of peroxide radicals ($•O_2H$) ($HO_2• \leftrightarrow H^+ + •O_2^-$). Herein, in this work, the role of •OH and $•O_2^-$ playing in reaction mechanism of E-Fenton process at different pH was further monitored by using the radical scavengers. Isopropanol (*i*-PrOH) has been described as the best hydroxyl radical quencher due to its high-rate constant reaction with •OH radical ($1.9 \times 10^9\ M^{-1}\ s^{-1}$) [29–31], while benzoquinone (BQ) is known for possessing high ability to trap superoxide anions by a simple electron transfer mechanism [32,33]. During this reaction, the amount of added radical scavenger was 1000 times greater than organic pollutant imidacloprid. As shown in Fig. 4A, about 51% and 4% inhibition were observed in TOC removal when *i*-PrOH and BQ were respectively added to acid solution at pH 3. The obvious inhibitory effect

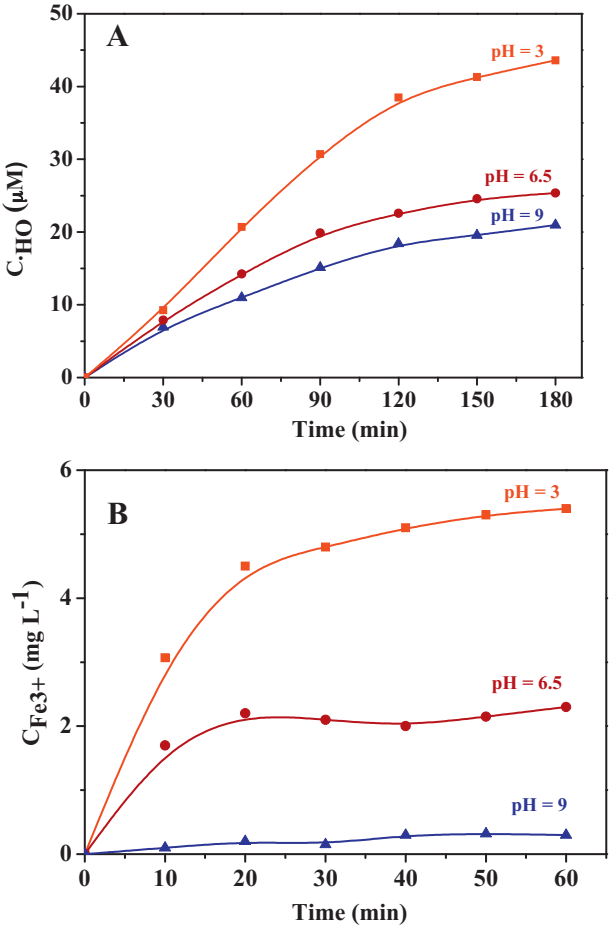

Fig. 3. The concentration of (A) generated ·OH on cathode and (B) leached Fe^{3+} during electro-Fenton process with Fe_3O_4@Fe_2O_3/ACA cathode over wide pH ranges.

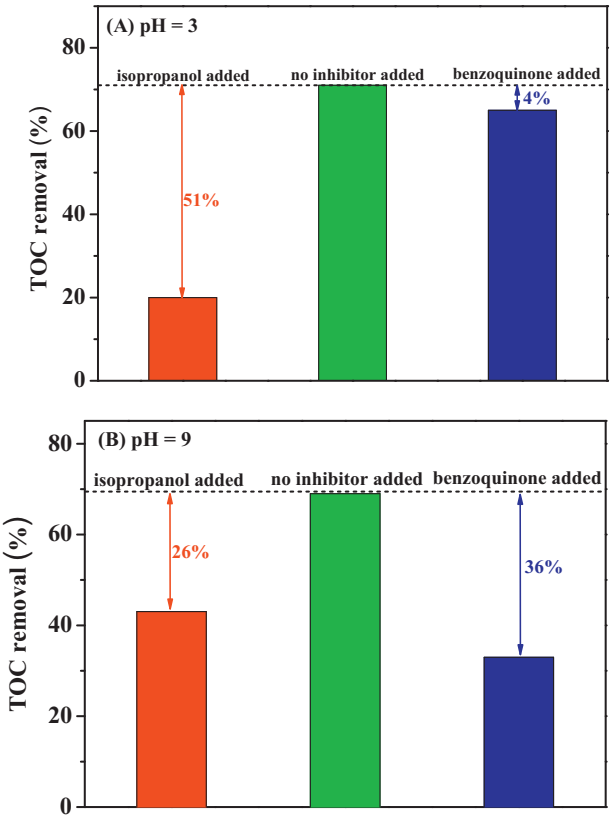

Fig. 4. Effect of radical inhibitors on TOC removal after reaction 60 min over wide pH ranges.

of isopropanol suggested that •OH radical presented as main participation under acid conditions. Fig. 4B presented the influence of quencher addition on imidacloprid degradation at pH 9. There was 36% and 26% decline in TOC removal in case BQ and *i*-PrOH were added, respectively. This result was categorical evidence to say that, under basic condition, the oxidants generated from the decomposition of H_2O_2 were mainly superoxide anions and to lesser extent were hydroxyl radicals.

3.3. *Surface properties and reactions of Fe_3O_4@Fe_2O_3/ACA cathode during E-Fenton oxidation reaction*

A clear correlation between the oxidants and pH values was found for better understanding the catalytic oxidation mechanism of Fe_3O_4@Fe_2O_3/ACA E-Fenton system. Another method often used to cast light on the mechanism of catalytic action is to search for relationship between the cathode activity and some other property of its surface.

The XRD pattern of fresh Fe_3O_4@Fe_2O_3/ACA cathode exhibited typical diffraction peaks characteristic carbon and iron oxide (see Fig. 5). However, the peak for iron oxide matches both magnetite (Fe_3O_4) and maghemite (γ-Fe_2O_3), suggesting the difficulty to distinguish this two phase only from the XRD analysis. Therefore, XPS measurements have to be consulted to unambiguously assign the crystal phase due to the high sensitivity to Fe^{2+} and Fe^{3+} cations [34]. In addition, the surface chemical compositions of samples before and after reaction under different pH values were deeply analyzed by XPS for investigating possible surface reactions. The Fe 2p and O1s peaks as well as the corresponding binding energies are depicted in Figs. 6 and 7, respectively.

Fig. 6 shows that the Fe 2p peak positions for fresh Fe_3O_4@Fe_2O_3/ACA cathode are at around 711.3 and 724.9 eV, with a right-shoulder and a shakeup satellite at 710.4 and 719.6 eV, respectively. After reaction in basic solution (pH 9), all the peaks mentioned above were kept the same expect for the right-shoulder at 710.4 eV, which was completely disappeared. The Fe 2p spectra of used cathode in acid solution was much weaker than the rest due to the low concentration of iron on the surface, nevertheless, the shape of obtained peaks was quite similar with fresh cathode. In order to get reliable Fe^{2+}/Fe^{3+} ratio and then understand what happed after reaction in basic solution, all Fe $2p_{3/2}$ spectra were fit

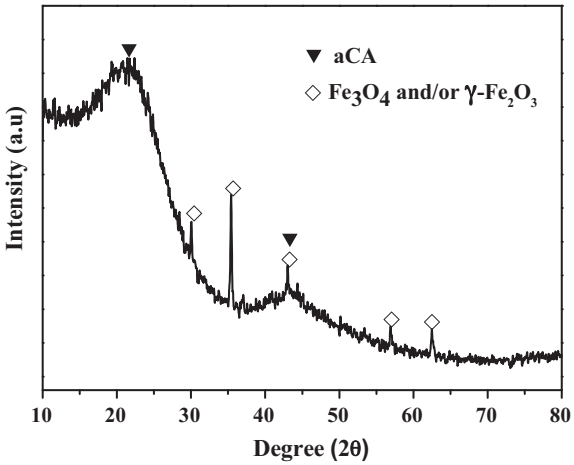

Fig. 5. XRD spectra of fresh Fe_3O_4@Fe_2O_3/ACA cathode.

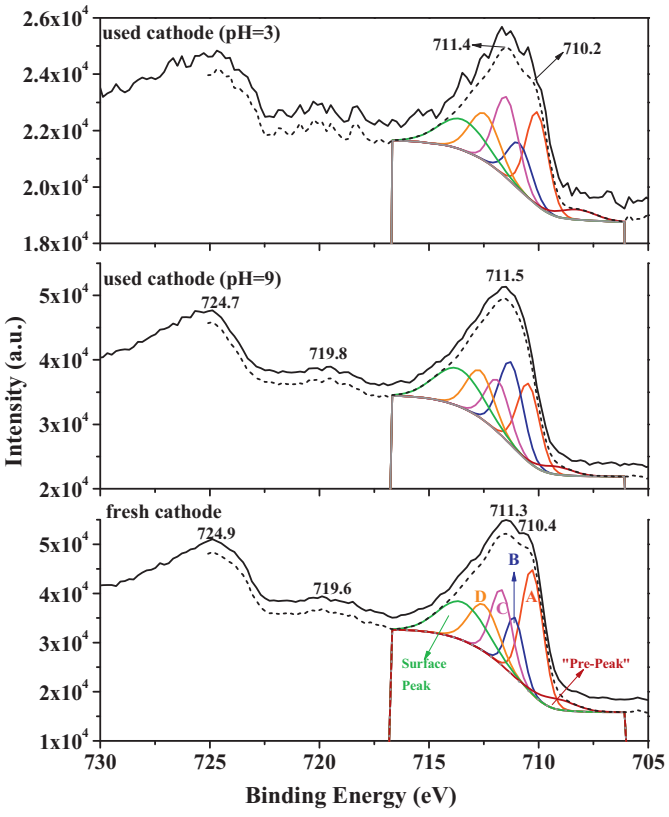

Fig. 6. Fe 2p XPS spectra of fresh and used Fe_3O_4@Fe_2O_3/ACA cathodes (experimental Fe 2p spectrum: black straight line, simulated Fe 2p spectrum by the contribution of iron from various compounds: black dotted line). The Fe^{3+} and Fe^{2+} multiplet peaks named by A, B, C and D have been labeled on the spectrum.

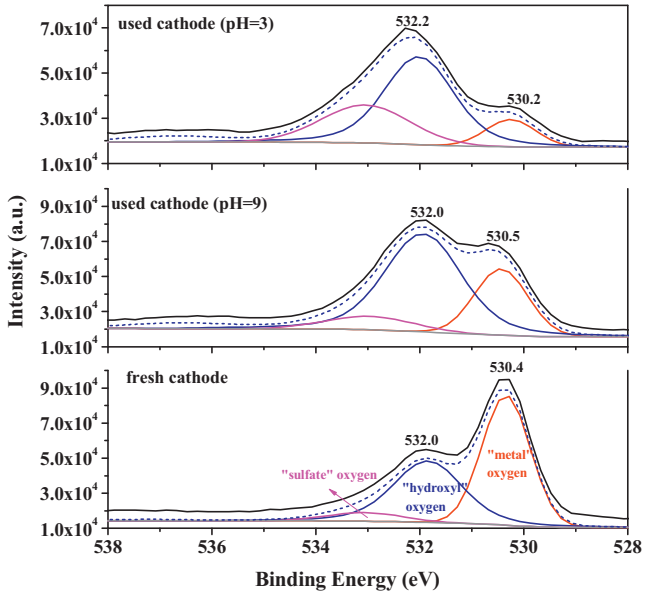

Fig. 7. O1s XPS spectra of fresh and used Fe_3O_4@Fe_2O_3/ACA cathodes (experimental O1s spectrum: black straight line, simulated O1s spectrum by the contribution of oxygen from various component oxides: black dotted line).

using GS multiplets as well as a high-binding energy (BE) surface peak and a low-BE "pre-peak" [35,36]. The high-BE surface peak reporting surface structures was added to fill the rest of envelope. While "pre-peak" on the low-BE side of the envelope was added to account for the formation of Fe ions with a lower than normal oxidation state by the production of defects in neighboring sites. The multiplet peaks referenced as A, B, C and D have been labeled on the spectrum in Fig. 6. According to literature [36], peak A was assigned to Fe(II) in Fe_3O_4, while peak B, C and D were corresponded to Fe(III) both in Fe_2O_3 and Fe_3O_4. The presence of a satellite peak at ~719 eV confirmed the presence of Fe_2O_3 on the surface of cathode. All these observations confirmed that fresh cathode was composed with mixed Fe_2O_3 and Fe_3O_4 phase, this is why we denoted Fenton catalysts as Fe3O4@Fe2O3. The disappearance of the right-shoulder at ~710.4 eV for used cathode at pH 9 would be explained by the transformation of peak A to peak B as depicted in Fig. 6, suggesting a new generation of surface Fe_2O_3 during E-Fenton process.

Meanwhile, O1s spectra of Fe_3O_4@Fe_2O_3/ACA before and after reaction were also recorded in Fig. 7. The peak of O1s was, in general, broad and complicated because of the overlapping contribution of oxygen from various oxides, which would be fitted by three peaks. The domain peak for fresh cathode at 530.4 eV is characteristic of oxygen in a metal oxide [37]. The peak at 532.0 eV is assigned to surface hydroxyl groups such as OH, H_2O and organic oxygen species, and the weak peak at around 533.1 eV is possible due to sulfate oxygen coming from Na_2SO_4 electrolyte. It is obviously that the oxygen content in Fe_3O_4@Fe_2O_3 decreased after reaction especially in acid condition, while the amount of surface–OH groups increased. That is to say, the surface of support ACA would be occupied by hydroxyl groups after E-Fenton oxidation.

The fact was further confirmed by the morphology of Fe_3O_4@Fe_2O_3/ACA cathode before and after reaction stages examined by SEM, as shown in Fig. 8A–C. The image of fresh cathode (see Fig. 8A) presented that iron oxide species with irregular micropolyhedral shape was well dispersed on the surface of ACA. After reaction in acidic solution (pH 3), the structure of Fe_3O_4@Fe_2O_3 particles remained the same. The corrosion of iron in acidic condition resulted in partial loss of surface particles (see Fig. 8B). Different from the fresh and used cathode at pH 3, besides the already known polyhedral-shaped species, new nanowires were detected for used cathode at pH 9 (see Fig. 8C). On the basis of XPS results, this new nanowire was most likely attributed to the regeneration of Fe_2O_3 on the surface of cathode during E-Fenton oxidation. The morphology of the used cathode after reaction at pH 9 was deeply analyzed by TEM, as shown in Fig. 9. Again, the new obtained nanowire with diameter around 55 nm was clearly next to the irregular circular shape particles. All the difference of morphological and surface iron content in acid and basic condition were related with its corresponding catalytic mechanism of solution based or surface based, which will be explained in detail in the following section about mechanism discussion.

Moreover, in order to provide complementary information about the variations of surface iron oxide species, FTIR measurements were carried out. Fig. 10 shows the FTIR spectra of fresh and used Fe_3O_4@Fe_2O_3/ACA cathodes as well as pure imidacloprid. In case of fresh Fe_3O_4@Fe_2O_3/ACA, a broad peak maximizing at 594 cm^{-1} with a right-hand shoulder at 630 cm^{-1} was obtained, due to the characteristic adsorption band of Fe—O bond of iron oxide [38]. As example, the spectra of more interested cathode, which was used in basic solution for 60 min, were depicted. The intensity of the bands at 594 and 630 cm^{-1} decreased a little. These results reflected to some content that most surface iron oxide specie remained the same in terms of composition and structure. Moreover, compared with pure imidacloprid sample as reference (inset of Fig. 10), no imidacloprid FTIR spectra was observed for used cathode, revealing that most of imidacloprid were decomposed after 60 min in E-Fenton system.

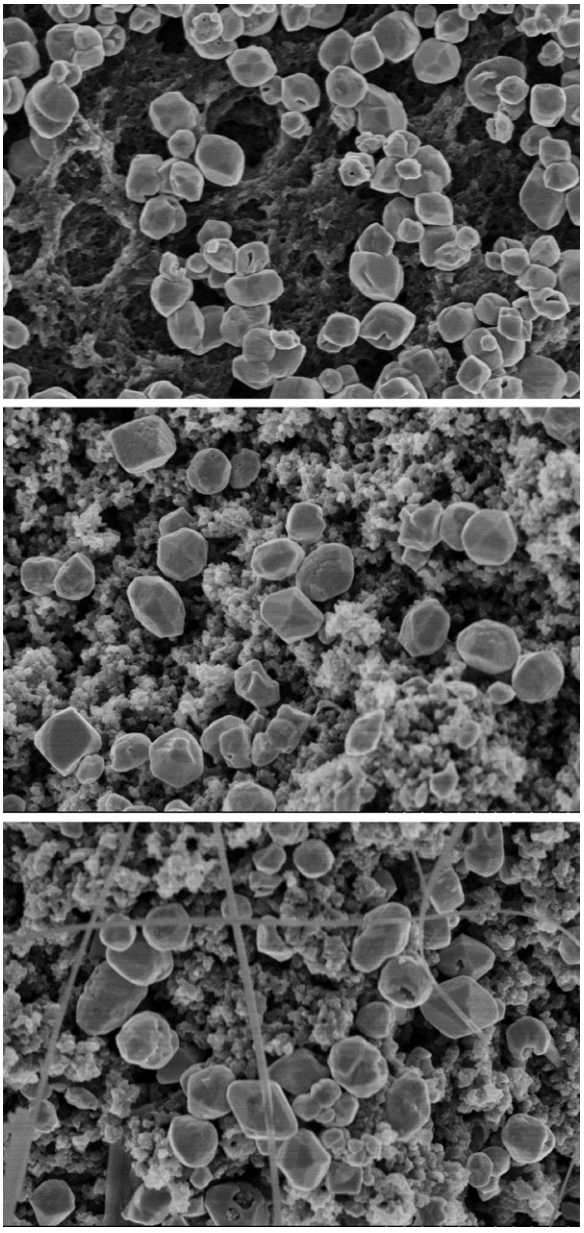

Fig. 8. SEM images of (A) fresh Fe_3O_4@Fe_2O_3/ACA cathode; (B) used Fe_3O_4@Fe_2O_3/ACA cathode in acidic solution (pH 3) after 60 min; (C) used Fe_3O_4@Fe_2O_3/ACA cathode in basic solution (pH 9) after 60 min.

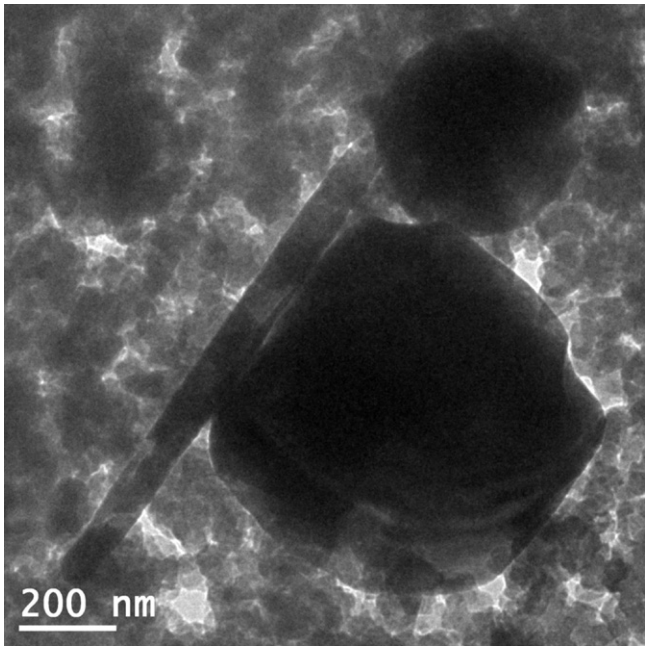

Fig. 9. TEM images of used Fe_3O_4@Fe_2O_3/ACA cathode in basic solution (pH 9) after 60 min.

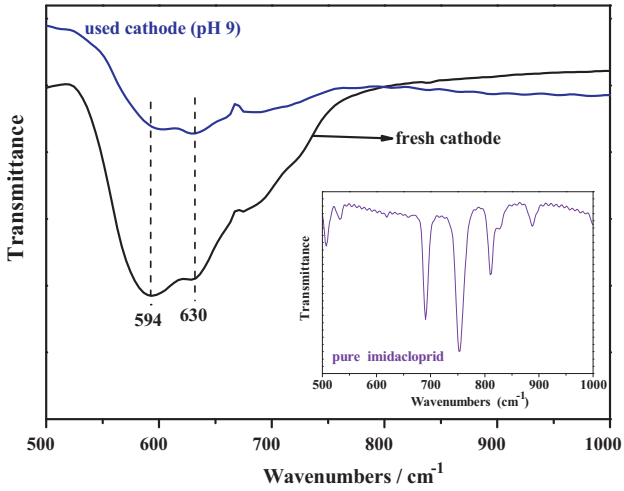

Fig. 10. FTIR spectra of Fe_3O_4@Fe_2O_3/ACA cathode before and after reaction 60 min at pH 9.

3.4. Oxidation mechanism of novel E-Fenton system in acidic and basic conditions

On the basis of the above results, possible pathways for degrading imidacloprid in E-Fenton process at pH 3 and 9 with Fe_3O_4@Fe_2O_3/ACA cathode were proposed, as depicted in Fig. 11A and B.

In acid solution, oxygen was adsorbed on the surface of Fe_3O_4@Fe_2O_3/ACA with high surface area of 2410 $m^2\ g^{-1}$ and then H_2O_2 was efficiently electro-generated thorough the reduction of oxygen on the cathode. Meanwhile, part of iron oxide was dissolved and immediately catalyzed the decomposition of H_2O_2 to generate hydroxyl radicals (•OH), presumably through a Haber–Weiss mechanism [39]. The main regeneration of Fe^{2+} ions would be obtained through a direct cathode reaction of electro-reduction of Fe^{3+} ions (Eq. (3)). In addition, since part of iron oxides particles were still remained on the surface of ACA, the high efficiency of this novel E-Fenton system could be also due to the better H_2O_2 activation to •OH by the surface of iron sites. Finally, the imidacloprid was degraded even mineralized by the generated hydroxyl radicals. During this process, the defects on cathode surface, produced by dissolved iron oxide, were occupied by hydroxyl groups. This is consisted with the XPS analysis results about O1s.

In basic solution, according to the obtained information, the catalytic mechanism of heterogeneous E-Fenton process was expected to be the interaction of H_2O_2 with Fe(III) and Fe(II) sites on the surface. Accordingly, a surface-based mechanism different from in acidic condition was proposed. As obviously shown in Fig. 11B, much more H_2O_2 were electro-generated on cathode surface since the optimum condition for the electro-generation of H_2O_2 is alkalinity, and then reacted with surface iron species (Fe(II)–OH and Fe(III)–OH sites). For Fe(II)–OH, it was interacted with H_2O_2 to form a precursor surface complex of H_2O_2 as shown in Eq. (5) [14,40], while for Fe(II)–OH, it was directly oxidized by H_2O_2 to become Fe(III)–OH (see Eq. (4)) and finally converted into new

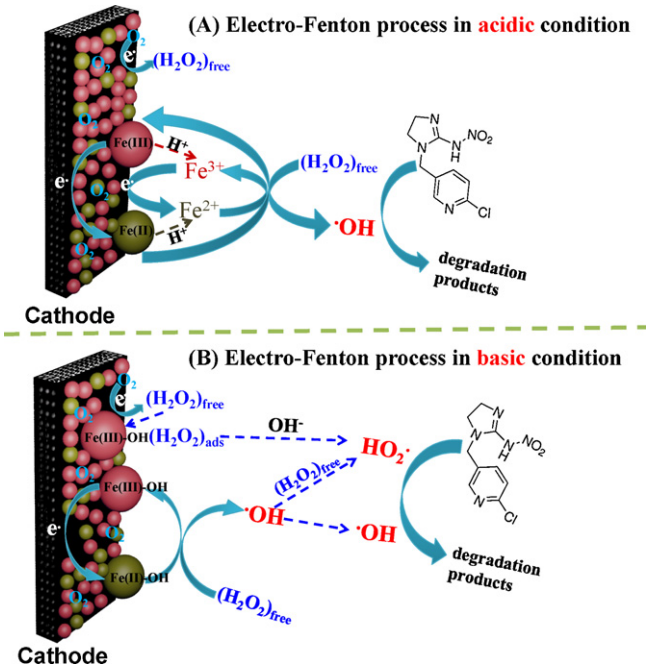

Fig. 11. Schematic illustration of electro-Fenton oxidation mechanisms with Fe_3O_4@Fe_2O_3/ACA cathode in (A) acidic and (B) basic condition.

Fe_2O_3 oxides, accompany with a potential in-situ recycling of iron oxide ($FeO{\cdot}Fe_2O_3 \rightarrow Fe_2O_3$) during E-Fenton process. Meanwhile, most of generated •OH in first stage would be ruined by considerable H_2O_2 through Eq. (6).

$$Fe(II)\text{–}OH + H_2O_2 \rightarrow Fe(III)\text{–}OH + {}^{\bullet}OH + H_2O \quad (4)$$

$$Fe(III)\text{–}OH + H_2O_2 \rightarrow Fe(III)\text{–}OH(H_2O_2)_{ads} \quad (5)$$

$$^{\bullet}OH + H_2O_2 \rightarrow HO_2{}^{\bullet} + H_2O \quad (6)$$

The surface H_2O_2 complex may further undergo a reversible ground-state electron transfer from ligand to metal (Eq. (7)), and then the successor complex would be deactivated through Eq. (8) to produce HO_2• oxidants [33]. Note that reaction 7 was especially active in basic solution since that formed protons (H^+) can immediately react with hydroxyls (OH^-) to promote the reaction rate. The reduced iron sites (Fe(II)–OH) then again reacted with H_2O_2 to regenerate Fe(III)–OH sites and produce •OH radical. This is why in E-Fenton process at pH 9 most of oxidants are $^{\bullet}O_2H$ ($^{\bullet}O_2^-$) oxidants not •OH radical, anyway, both of oxidants finally attack imidacloprid pollutants.

$$Fe(III)\text{–}OH(H_2O_2)_{ads} \rightarrow Fe(II)\text{–}OH(HO_2{}^{\bullet})_{ads} + H^+ \quad (7)$$

$$Fe(II)\text{–}OH(HO_2{}^{\bullet})_{ads} \rightarrow Fe(II)\text{–}OH + HO_2{}^{\bullet} \quad (8)$$

Finally, a reasonable oxidation mechanism of novel E-Fenton system with composite cathode at different pH values was successfully described in terms of typical a Haber–Weiss mechanism and surface reactions including the formation, deactivation of H_2O_2 complex and catalytic decomposition of H_2O_2, which depends on its own reaction conditions.

4. Conclusions

This study reported a heterogeneous electro-Fenton system based on a novel Fe_3O_4@Fe_2O_3/ACA composite cathode. This system was more efficiently degrade imidacloprid than those with Fe^{2+} as the iron reagents at its optimum pH 3. In addition, it would be worked very well over a wide pH ranges from 3 to 9 without sacrificing efficiency. The removal of imidacloprid and TOC achieved around 90% within 30 and 60 min, respectively. This efficiency was strongly related with the nature of cathode. The ACA, possessing high surface area of 2410 $m^2\ g^{-1}$ and multiplicated porosities composed of micropores and mesopores with size respectively centered at 1.7 and 3.5, worked not only as cathode for efficiently in-situ electro-generating H_2O_2, but also as Fenton catalyst support for improving its catalytic performance. In addition, the composite iron oxides in terms of hematite and magnetite with high activity were well dispersed on the surface of electrode, as indicated by XPS and SEM. The corresponding oxidation mechanisms of E-Fenton process with novel Fe_3O_4@Fe_2O_3/ACA cathode at different pH ranges was proposed through the role of participant oxidants, surface properties and reactions by the comprehensive characterizations. In acidic solution, it followed a Haber–Weiss mechanism that the dissolved iron ions and surface Fe(II) sites immediately reacted with H_2O_2 to generate hydroxyl radicals (•OH). While in basic solution, it adhered to the formation, deactivation of H_2O_2 complex with surface Fe(III) sites and the catalytic decomposition of H_2O_2 with Fe(II) sites, producing both superoxide anion ($^{\bullet}O_2^-$/HO_2•) and hydroxyl radicals (•OH). For respective, this promising E-Fenton process has great development potential for practical wastewater treatment since its high efficiency and friendly working condition especially at neutral pH. And the understanding of its catalytic oxidation mechanism may lead to the development of more efficient Fenton catalysts and methods.

Acknowledgements

This work was supported jointly by the National Natural Science Foundation PR China (Project No. 21077077), Shanghai Educational Development Foundation (Project No. 2011CG19) and the Program for Young Excellent Talents in Tongji University (Project No. 2010KJ063).

References

[1] C. Walling, K. Amarnath, Journal of the American Chemical Society 104 (1982) 1185–1189.
[2] F. Chen, W.H. Ma, J.J. He, J.C. Zhao, Journal of Physical Chemistry A 106 (2002) 9485–9490.
[3] F.J. Rivas, F.J. Beltrán, J. Frades, P. Buxeda, Water Research 35 (2001) 387–396.
[4] R. Konecny, Journal of Physical Chemistry B 105 (2001) 6221–6226.
[5] C.K. Duesterberg, T.D. Waite, Environmental Science and Technology 40 (2006) 4189–4195.
[6] J.Y. Feng, X.J. Hu, P.L. Yue, Environmental Science and Technology 38 (2004) 269–275.
[7] S. Navalon, M. Alvaro, H. Garcia, Applied Catalysis B: Environmental 99 (2010) 1–26.
[8] G.Q. Zhang, F.L. Yang, M.M. Gao, L.F. Liu, Journal of Physical Chemistry C 112 (2008) 8957–8962.
[9] Z.H. Ai, H.Y. Xiao, T. Mei, J. Liu, L.Z. Zhang, K.J. Deng, J.R. Qiu, Journal of Physical Chemistry C 112 (2008) 11929–11935.
[10] Z.H. Ai, T. Mei, J. Liu, J.P. Li, F.L. Jia, L.Z. Zhang, J.R. Qiu, Journal of Physical Chemistry C 111 (2007) 14799–14803.
[11] E. Brillas, I. Sirés, M.A. Oturan, Chemical Reviews 109 (2009) 6570–6631.
[12] C.A. Martínez-Huitle, E. Brillas, Applied Catalysis B: Environmental 87 (2009) 105–145.
[13] B.R. Petigara, N.V. Blough, A.C. Mignerey, Environmental Science and Technology 36 (2002) 639–645.
[14] S.S. Lin, M.D. Gurol, Environmental Science and Technology 32 (1998) 1417–1423.
[15] N.Y. Lee, R.M. Lago, J.L.G. Fierro, J. González, Applied Catalysis A-General 215 (2001) 245–256.
[16] V. Kitsiou, N. Filippidis, D. Mantzavinos, I. Poulios, Applied Catalysis B: Environmental 86 (2009) 27–35.
[17] U. Černigoj, U.L. Štangar, P. Trebše, Applied Catalysis B: Environmental 75 (2007) 229–238.
[18] S. Malato, J. Blanco, J. Cáceres, A.R. Fernández-Alba, A. Agüera, A. Rodríguez, Catalysis Today 76 (2002) 209–220.
[19] A. Cabrera Reina, L. Santos-Juanes Jordá, J.L. Garcia Sánchez, J.L. Casas López, J.A. Sánchez Pérez, Applied Catalysis B: Environmental 119–120 (2012) 132–138.
[20] M. Wu, Y. Jin, G. Zhao, M. Li, D. Li, Environmental Science and Technology 44 (2010) 1780–1785.
[21] Y. Jin, G. Zhao, M. Wu, Y. Lei, M. Li, X. Jin, Journal of Physical Chemistry C 115 (2011) 9917–9925.

[22] B.Y. Geng, J.Z. Ma, J.H. You, Crystal Growth and Design 8 (2008) 1443–1447.
[23] S. Fukui, Y. Hanasaki, H. Ogawa, Journal of Chromatography A 630 (1993) 187–193.
[24] C. Tai, J.F. Peng, J.F. Liu, G.B. Jiang, H. Zou, Analytica Chimica Acta 527 (2004) 73–80.
[25] J. Gao, G. Zhao, M. Liu, D. Li, Journal of Physical Chemistry A 113 (2009) 10466–10473.
[26] E. Isarain-Chavez, C. Arias, P.L. Cabot, F. Centellas, R.M. Rodriguez, J.A. Garrido, E. Brillas, Applied Catalysis B: Environmental 96 (2010) 361–369.
[27] F. Duarte, F.J. Maldonado-Hódar, A.F. Pérez-Cadenas, L.M. Madeira, Applied Catalysis B: Environmental 85 (2009) 139–147.
[28] J. Zhang, J. Zhuang, L. Gao, Y. Zhang, N. Gu, J. Feng, D. Yang, J. Zhu, X. Yan, Chemosphere 73 (2008) 1524–1528.
[29] W.P. Kwan, B.M. Voelker, Environmental Science and Technology 38 (2004) 3425–3431.
[30] Y. Chen, S. Yang, K. Wang, L. Lou, Journal of Photochemistry and Photobiology A: Chemistry 172 (2005) 47–54.
[31] S. Rafqah, P. Wong-Wah-Chung, S. Nelieu, J. Einhorn, M. Sarakha, Applied Catalysis B: Environmental 66 (2006) 119–125.
[32] L. Cermenati, P. Pichat, C. Guillard, A. Albini, Journal of Physical Chemistry B 101 (1997) 2650–2658.
[33] M. Stylidi, D.I. Kondarides, X.E. Verykios, Applied Catalysis B: Environmental 47 (2004) 189–201.
[34] T. Fujii, F. Groot, G. Sawatzky, F. Voogt, T. Hibma, K. Okada, Physical Review B 59 (1999) 3195–3202.
[35] J.R. Mycroft, H.W. Nesbitt, A.R. Pratt, Geochimica et Cosmochimica Acta 59 (1995) 721–733.
[36] A.P. Grosvenor, B.A. Kobe, M.C. Biesinger, N.S. McIntyre, Surface and Interface Analysis 36 (2004) 1564–1574.
[37] Z. Ai, L. Lu, J. Li, L. Zhang, J. Qiu, M. Wu, Journal of Physical Chemistry C 111 (2007) 7430–7436.
[38] G. Zhao, J. Feng, Q. Zhang, S. Li, H. Chen, Chemistry of Materials 17 (2005) 3154–3159.
[39] J.J. Pignatello, E. Oliveros, A. Mackay, Environmental Science and Technology 36 (2006) 1–84.
[40] A.L.T. Pham, F.M. Doyle, D.L. Sedlak, Environmental Science and Technology 46 (2012) 1055–1062.